



Chemokine-like factor 1 (CKLF1) is expressed in myocardial ischemia injury *in vivo* and *in vitro*

JULING FENG^{1,3}; HAODONG CHEN¹; YANGBO LIU¹; QIDI AI¹; YANTAO YANG¹; LEI ZHAO⁴; SHIFENG CHU^{2,*}; NAIHONG CHEN^{1,2,*}

¹ School of Pharmacy, Department of Pharmacy, Hunan Engineering Technology Center of Standardization and Function of Chinese Herbal Decoction Pieces, Hunan University of Chinese Medicine, Changsha, 410208, China

² Department of Pharmacology, State Key Laboratory of Bioactive Substances and Functions of Natural Medicines, Institute of Materia Medica & Neuroscience Center, Chinese Academy of Medical Sciences and Peking Union Medical College, Beijing, 100050, China

³ Department of Diagnostics Research Lab of Translational Medicine, Hengyang Medical College, University of South China, Hengyang, 421001, China

⁴ Department of Gastrointestinal Surgery, The First Affiliated Hospital, Hengyang Medical College, University of South China, Hengyang, 421001, China

Key words: Chemokine-like factor 1, Overexpression, Myocardial infarction

Abstract: Introduction: Chemokine-like factor 1 (CKLF1) is a chemokine that is overexpressed in several diseases. Our previous findings revealed a significant increase in CKLF1 expression in the ischemic brain, suggesting its potential as a therapeutic target for ischemic stroke. **Methods:** In this study, we examined the expression dynamics of CKLF1 in both *in vivo* and *in vitro* models of ischemic cardiac injury. Myocardial infarction (MI) was induced *in vivo* by ligation of the left anterior descending artery (LAD) of the rat heart. The levels of CKLF1, Creatine Kinase MB Isoenzyme (CK-MB), and Lactate dehydrogenase (LDH) in the serum were detected using Enzyme-linked immunosorbent assay (ELISA). The expression of CKLF1 in the infarcted area was detected by immunohistochemistry, immunofluorescence, quantitative PCR (qPCR), and Western blotting (WB). H9C2 and AC16 cardiomyocytes cultured *in vitro* were subjected to oxygen and glucose deprivation (OGD). LDH was used to detect cell damage, and CKLF1 expression was detected by qPCR and WB. **Results:** CKLF1 mRNA and protein expression were significantly increased in h9c2 cells at 1.5 h and in AC16 cells at 4 h after OGD. The serum CK-MB in rats increased significantly on the first day after infarction, while the LDH concentration increased significantly on the third day after infarction. CKLF1 blood levels significantly increased on the first day following MI in rats. CKLF1 expression notably increased in the infarct area on days 1, 3, and 7 post-MI. In MI tissue, CKLF1 colocalizes with cardiomyocytes, macrophages, and neutrophils. **Conclusion:** CKLF1 was substantially expressed during myocardial ischemia injury both *in vivo* and *in vitro* and was colocalized with macrophages and neutrophils, indicating that CKLF1 is expected to be a biomarker and a drug target for the treatment of myocardial infarction.

List of abbreviations

CKLF1	Chemokine-like factor 1	OA	Osteoarthritis
OGD	Oxygen and glucose deprivation	AS	Ankylosing spondylitis
MCP	Monocyte chemoattractant protein 1	TGF- β	Transforming growth factor- β
CCR2	CC chemokine receptor 2	TNF- α	Tumor necrosis factor- α
CCR4	CC chemokine receptor 4	CK-MB	Creatine kinase MB isoenzyme
RA	Rheumatoid arthritis	LDH	Lactate dehydrogenase
		MMPs	Matrix metalloproteinases

*Address correspondence to: Shifeng Chu, chushifeng@imm.ac.cn; Naihong Chen, chennh@imm.ac.cn

#Shifeng Chu and Naihong Chen contributed equally to this work
Received: 24 January 2024; Accepted: 09 April 2024;
Published: 10 June 2024

Introduction

Acute myocardial infarction (AMI) is one of the leading causes of death worldwide, and its mortality rate is increasing annually [1–3]. AMI occurs when the coronary



artery suddenly becomes blocked, leading to diminished blood flow, which results in myocardial necrosis. An inflammatory response induced by necrotic myocardium leads to the production and release of numerous cytokines and chemokines [4,5]. Chemokines play a vital role in the initial inflammatory response to infarction [5,6]. Chemokines attract many intrinsic cardiac mononuclear macrophages, lymphocytes, and neutrophils to infiltrate infarcted cardiomyocytes, facilitating the gradual removal of dead cells and matrix debris [7,8]. Chemokine-induced leukocytes remove dead cells and matrix debris early in the inflammatory response; however, excessive, prolonged, and persistent inflammation can cause significant harm and promote undesirable remodeling. Growing evidence has demonstrated that most chemokines can influence cardiac repair and remodeling by supporting the development of new blood vessels, affecting fibroblast conversion to myofibroblasts, interacting with matrix metalloproteinases (MMPs), and modulating collagen production [5].

Chemokine-like factor 1 (CKLF1), is a newly identified chemokine family member with a molecular weight of approximately 8–13 kDa [9]. Numerous studies have revealed that CKLF1 performs a variety of biological activities, including leukocyte chemotaxis, and stimulates the proliferation and differentiation of many cells. CKLF1 has a wide range of chemotactic effects on leukocytes and participates in inflammatory responses and autoimmune diseases [9]. A previous study showed that CKLF1 gene transfer reduced myocardial infarct size and improved cardiac function in rats after myocardial infarction [10]. Additionally, research has demonstrated that CKLF1 may direct mouse peripheral blood CD34+ cells following myocardial infarction to the infarcted region and heal the myocardium [11]. Our previous studies have shown that CKLF1 expression is significantly upregulated in the ischemic brain during stroke, whereas downregulation of CKLF1 reduces neutrophil infiltration in the infarct area [12], inhibits inflammatory responses [13], and reduces infarct size and the occurrence of myocardial infarction complications after stroke [14].

To accurately diagnose the condition and investigate its mechanism, it is helpful to understand how CKLF1 is expressed during myocardial infarction. There is still uncertainty regarding CKLF1 expression levels in myocardial infarction models. The purpose of our study was to demonstrate that CKLF1 is expressed in myocardial infarction both *in vitro* and *in vivo*. We showed that myocardial infarction dramatically increased CKLF1 expression.

Materials and Methods

Cell culture and oxygen and glucose deprivation (OGD) treatment

Rat embryonic cardiomyocyte H9c2 cells and human cardiomyocyte AC16 cells were obtained from Procell (Wuhan, China). High-glucose Dulbecco's modified Eagle's medium (DMEM) (Sigma, D5796, St. Louis, USA) supplemented with 10% fetal bovine serum (FBS) (Sigma, F0193, Shanghai, China) was used to cultivate the cells at 37°C in a 5% CO₂ environment.

To simulate the interruption of blood flow after myocardial infarction, H9c2 and AC16 cells were grown in serum-, glucose-, and sodium pyruvate-free DMEM (Procell Life Science & Technology Co. Ltd., PM 150270, Wuhan, China) in an anaerobic chamber at 37°C with 95% N₂ and 5% CO₂ for OGD treatment.

Cell damage analysis

The amount of lactate dehydrogenase (LDH) released into the cell culture supernatant was used to gauge the extent of cell damage. Following appropriate treatment of the cardiomyocytes, 50 mL of the cell culture supernatant was removed and run through automated biochemical equipment along with the LDH test reagent (Sangon Biotech, 100020050, Shanghai, China). An automatic program for biochemical equipment (Toshiba, TBA40F, Japan) was used for LDH analysis, and the findings were recorded.

Animals

Male Sprague-Dawley rats weighing 250–280 g were purchased from Vital River Laboratory Animal Technology Co., Ltd. (Beijing, China), and housed in cages at a comfortable temperature of 22°C and 40%–60% humidity. Rats had unrestricted access to food and water in the laboratory. All operations were carried out in line with the National Institutes of Health Guide for the Care and Use of Laboratory Animals and were authorized by the Peking Union Medical College and Chinese Academy of Medical Sciences Animal Care Committee (number: 00007889).

Establishment of the myocardial infarction model

To induce anesthesia, the rats were anesthetized with 2% isoflurane. The skin and thyroid were separated at the level of the thyroid cartilage. Tracheotomy was performed on the second and third tracheal rings, endotracheal intubation was completed, and then the rat trachea was linked. The ventilator respiration rate and respiratory ratio were set to 90 per min and 1:1, respectively. Isoflurane was adjusted to 1.5%, N₂ to 70%, and O₂ to 30% for maintenance purposes. The skin, pectoralis major, and serratus anterior muscles were separated in the third intercostal space. At the end of expiration, the pleura was punctured, a 6–0 suture was used to ligate the region 3–4 mm below the junction between the aortic arch and the left atrial appendage, and the chest was then closed. The ligated rats were used as the model group, with 3 rats in each group. Sham rats were threaded but not ligated, with 3 rats in each group. Serum and heart samples were collected 1, 3, and 7 days after the procedure.

Tetrazolium chloride (TTC) staining

The rat heart was removed and immediately frozen for 10 min at –80°C. The heart was serially sectioned from the base to the apex at 1 mm intervals. The slices were exposed to a 1.5% 2,3,5-triphenyltetrazolium chloride (TTC) (Sigma, T8877, Shanghai, China) solution for 20 min. ImageJ software (National Institutes of Health, Maryland, USA) was used to evaluate the degree of infarct. Infarct rate (%) = total infarct area/total area × 100.

Hematoxylin-eosin (HE) staining

After the damage, the rats wore masks and were anesthetized with 2% isoflurane. Following perfusion with phosphate-buffered saline and 4% paraformaldehyde (Sigma, 441244, Shanghai, China), the hearts were removed and preserved in 4% paraformaldehyde, and the retrieved heart was treated according to established protocols in paraffin-coated and graded alcohols as well as xylene. The paraffin-embedded slices were serially sectioned at 5 mm intervals. The slides were stained with hematoxylin and eosin for 20 and 2 min, respectively, and examined under a microscope (Olympus, CKX41, Tokyo, Japan).

Immunofluorescence staining and immunohistochemistry

CKLF1 expression in the myocardium was examined using immunohistochemistry and immunofluorescence staining. Antigen retrieval was performed by boiling the heart sections in 0.01 mol/L citrate acid buffer at 100°C for 5 min. Sections of heart tissue were added to 3% H₂O₂ for 10 min at room temperature before immunohistochemistry to stop endogenous peroxidase activity. Then, 5% bovine serum (Sigma, V900933, Shanghai, China) was added, and the samples were allowed to sit for 30 min at room temperature. Primary antibodies against CKLF1 (Abcam, ab180512, Massachusetts, USA, 1:200), MHC (Abcam, ab37484, Massachusetts, USA, 1:200), CD68 (Abcam, ab303565, Massachusetts, USA, 1:200), and MPO (Abcam, ab208670, Massachusetts, USA, 1:200) were added and incubated overnight at 4°C. A secondary antibody and Hoechst 333 (Proteintech, CL594-67243, Wuhan, China, 1:1000) were added, and the cells were incubated for 2 h at room temperature. Finally, the sections were imaged using a confocal laser scanning microscope (Leica, TCS SP2, Solms, Germany) for immunofluorescence staining or an immunohistochemical staining microscope (Olympus, CKX41, Tokyo, Japan). The photos were examined using Image-Pro Plus 6.0. For colocalization analysis, we selected cells in the picture for the presence of colocalization, and ImageJ was used for colocalization analysis of the selected portion, and the target protein trends consistently indicated the presence of colocalization.

Determination of the serum creatine kinase MB isoenzyme (CK-MB) concentrations in rats

The concentration of CK-MB in the rat serum was evaluated using a rat CK-MB enzyme-linked immunosorbent assay (ELISA) Kit (Sangon Biotech, D731144, Shanghai, China) according to the manufacturer's instructions.

ELISA

The concentration of CKLF1 in the rat serum was evaluated using a rat CKLF1 ELISA kit (Jianglai, JL47923, Shanghai, China) according to the manufacturer's instructions.

Quantitative PCR (qPCR)

Quantitative PCR was used to evaluate CKLF1 expression. H9c2 and total myocardial RNA were extracted using TRIzol reagent (Invitrogen Carlsbad, 15596018CN, CA, USA) according to the manufacturer's instructions. A microplate reader (Implen, NanoPhotometer N60, Munich,

Germany) was used to quantify the amount of RNA present, and reverse transcription was permitted if the purity of the RNA had 260/280 nm absorbance between 1.8 and 2.1. Reverse cDNA was prepared using 1 µg of RNA and the TransScript One-Step gDNA Removal and cDNA Synthesis SuperMix Kit (TransGen, AT311-02, Beijing, China). A TransStart Tip Green qPCR Supermix kit (TransGen, AQ142-21, Beijing, China) was used to amplify the QPCR cDNA for real-time quantification. The results were analyzed using the $2^{-\Delta\Delta CT}$ method, with β -actin serving as the reference gene. The primers used for rat CKLF1 were F-5'CGTAGACCATCAGCCCTTCTG3' and R-5'TCAGGAA CCAAACACCCCTC3'; the primers used for β -actin were F-5'TCAGGTCATCACTAT CGGCAAT 3', and R-5'AAA GAAAGGGTGTAACGCA 3'.

Western blotting

Total protein was extracted from cells and tissues using RIPA (Beyotime, P0013B, Shanghai, China) buffer supplemented with 1% phenyl-methane sulfonyl fluoride (PMSF) (Beyotime, ST506-2, Shanghai, China). Protein concentrations were measured using the BCA Protein Assay Kit (Applygen Technologies, P1511-3, Beijing, China), and equivalent amounts of protein were transferred to polyvinylidene fluoride (PVDF) membranes (Merck millipore, 03010040001, Massachusetts, USA) after separation on 12% (w/v) SDS-PAGE gels. The membranes were subsequently labeled with primary antibodies against CKLF1 (Abcam, ab180512, Massachusetts, USA, 1:500) at 4°C overnight, then blocked with 5% Bull Serum Albumin (BSA) in Tris-buffered saline + Tween-20 (TBST) 2 h. GADPH (Sanying, 60004-1-I g, Wuhan, China) was used as an endogenous control. The membranes were cleaned before incubation for 2 h at room temperature with a secondary antibody (Sanying, HRP-20758, Wuhan, China). Bands on the membranes were detected using an improved chemiluminescence plus detection system (Molecular Devices, Lmax, CA, USA).

Statistical analysis

All the data are presented as the mean \pm SEM, and GraphPad Prism 7.0 (GraphPad Software), a statistical software, was used to analyze the data. The Bonferroni multiple comparison test in two-way ANOVA, Tukey's test in one-way ANOVA, and Student's *t*-test (when comparing two sets of data) were employed in this study for statistical analysis. Statistical significance was defined as $p < 0.05$.

Results

Hypoxia induces cell damage in cardiomyocytes

H9c2 and AC16 cardiomyocytes were subjected to oxygen and glucose deprivation (OGD) for different durations to simulate hypoxia. Lactate dehydrogenase (LDH) content was used to assess the effect of OGD on cell damage. Treatment of cardiomyocytes with OGD resulted in a visibly aberrant morphology (Figs. 1A and 1B), and the amount of LDH in the cell supernatant significantly increased in a time-dependent manner. When OGD was applied to AC16 cells

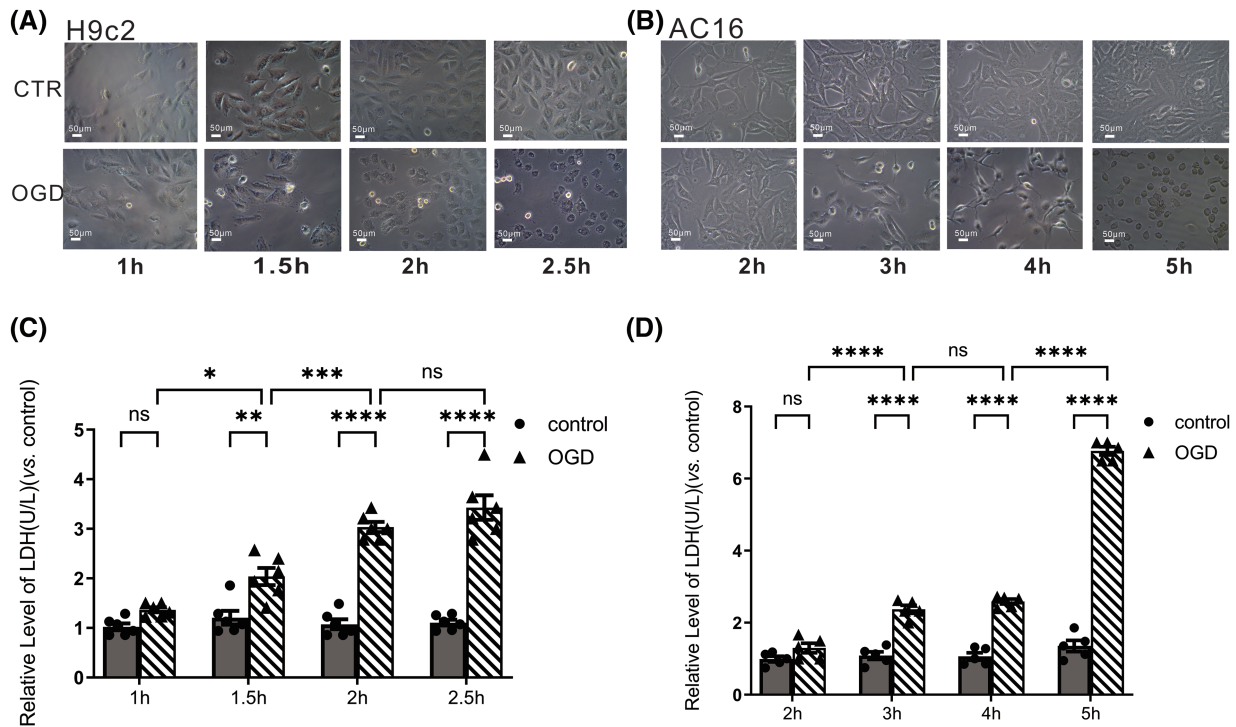


FIGURE 1. OGD induced H9c2 and AC16 cell damage. (A and B) Morphological changes of cardiomyocytes after OGD. Scale bar = 50 μm . (C and D) LDH content was used to assess cell injury. Data represent the mean \pm SEM ($n = 5$ and 6). * $p < 0.05$, ** $p < 0.01$, *** $p < 0.001$, **** $p < 0.0001$ vs. control groups, respectively. ns: no statistical significance.

for 3 h and H9c2 cells for 1.5 h, H9c2, and AC16 cells sustained significant damage. Furthermore, when H9c2 cells were subjected to OGD for 1.5 h and AC16 for 3 h, the LDH content doubled (Figs. 1C and 1D). These findings indicated that OGD-induced hypoxia may contribute to the destruction of H9c2 and AC16 cells.

OGD increased the expression of chemokine like factor 1 (CKLF1) in cardiomyocytes

Our previous study revealed that the expression of CKLF1 mRNA and protein in neurons increased after OGD/R [15]. To determine whether the expression of CKLF1 in cardiomyocytes changes under OGD conditions, Quantitative PCR (qPCR) and Western blotting were used to analyze the mRNA and protein levels of CKLF1. Cardiomyocytes were investigated by qPCR 10 h after OGD and Western blotting 12 h after OGD. The data confirmed that CKLF1 mRNA (Figs. 2A and 2B) and protein levels (Figs. 2C and 2D) increased significantly after OGD in both H9c2 and AC16 cells. This finding suggested that CKLF1 expression was upregulated in cardiomyocytes after OGD.

Alterations in myocardial enzyme levels and assessment of infarct size after myocardial infarction in rats

A rat Acute myocardial infarction (AMI) model was established for *in vivo* research. The area of myocardial infarction was measured using Tetrazolium chloride (TTC) staining. Usually, after TTC staining, the infarcted area of the rat heart was gray white and the normal area was red. TTC staining was performed 1, 3, and 7 days after myocardial infarction. Compared to those of the sham group, the infarct areas of the MI group were considerably

greater, at 12.32%, 23.23%, and 37.94%, respectively ($p < 0.001$) (Figs. 3A and 3C). Myocardial damage was evaluated using H&E staining. There were many necrotic myocardial cells, damaged and disorganized myocardial fibers, and significant infiltration of inflammatory cells in the infarcted region and border, indicating that myocardial ischemia occurred in the MI group (Fig. 3B). One day after myocardial infarction, the level of Creatine Kinase MB Isoenzyme (CK-MB) in rat serum was significantly greater than that in the sham operation group ($p < 0.0001$) (Fig. 3D). Suggesting the presence of acute myocardial injury. However, there was no difference between the two groups on the third day, which was mainly related to the repair of cardiomyocytes and the removal of necrotic material. LDH levels were not significantly different between the two groups one day after myocardial infarction but were significantly greater than those in the sham surgery group on the third day ($p < 0.01$) (Fig. 3E). These results demonstrate that myocardial damage occurs in a successful rat model of myocardial infarction.

CKLF1 was overexpressed in the rat model of AMI

To examine the expression of CKLF1 in the AMI rat model, immunohistochemical staining, ELISA, and Western blotting were performed. The expression of CKLF1 in the infarct area and, notably, the border zone dramatically increased compared to that in the sham group at 1, 3, and 7 days following myocardial infarction in rats, according to immunohistochemistry (Figs. 4A and 4B). On the first day following myocardial infarction, CKLF1 levels in rat serum dramatically increased in comparison to those in the sham group, but there was no change on days 3 or 7 (Fig. 4C).

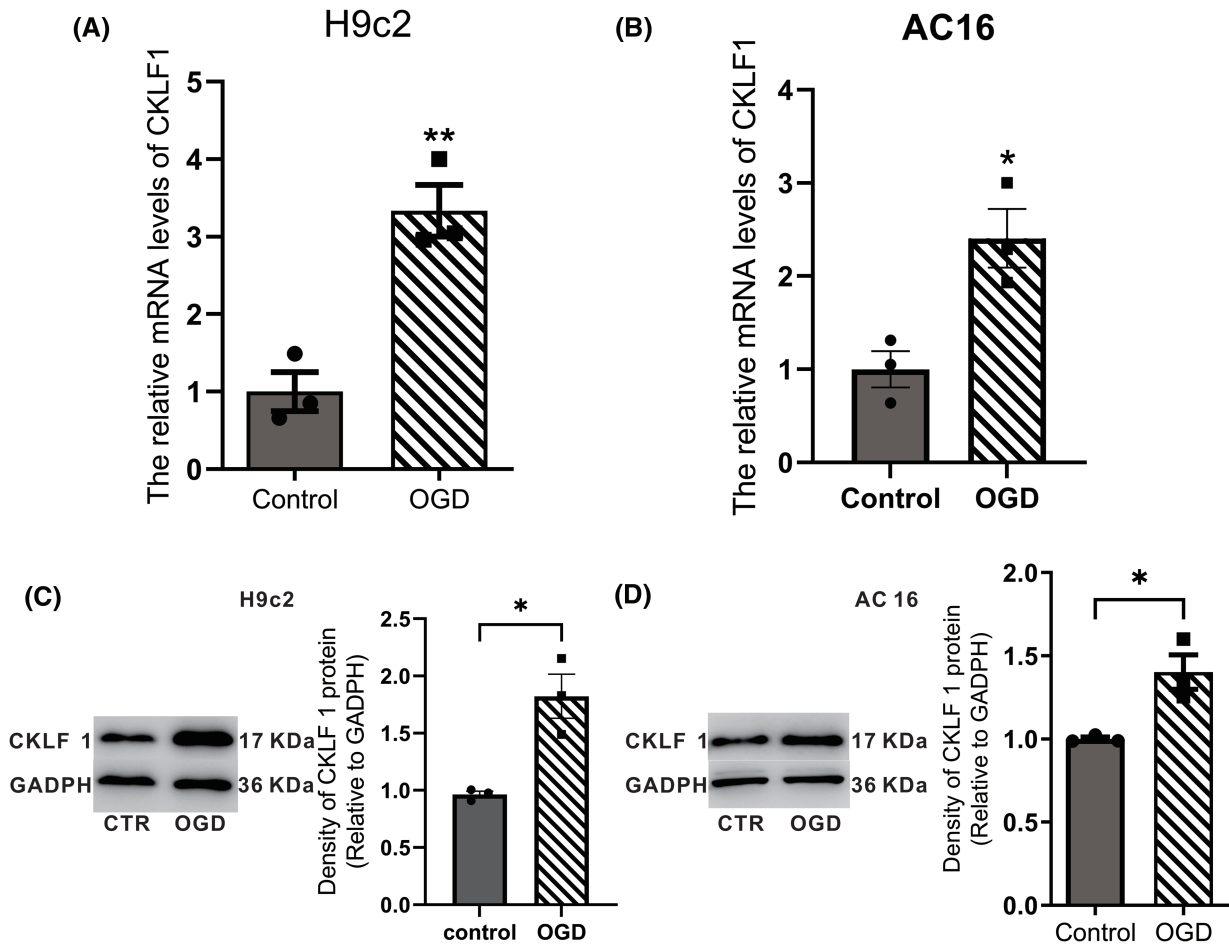


FIGURE 2. The expression of CKLF1 after OGD in H9c2 and AC16 cells. (A and B) CKLF1 mRNA expression in cardiomyocytes after OGD was detected using qPCR. (C and D) Western blotting was used to detect the expression of CKLF1 protein in cardiomyocytes after OGD. Data represent the mean \pm SEM ($n = 3$). * $p < 0.05$, ** $p < 0.01$ vs. control groups, respectively.

Western blotting also showed that CKLF1 expression steadily increased at 1, 3, and 7 days following infarction in comparison with that in the sham group (Fig. 4D).

CKLF1 colocalized with cardiomyocytes, macrophages, and neutrophils in the infarct region

To confirm the origin of CKLF1 in the infarct region after myocardial infarction, dual immunofluorescence labeling was performed. Immunofluorescence results showed that the fluorescence intensity of CKLF1 was significantly increased in the border zone of the myocardial infarction on days 1, 3, and 7 (Fig. 5A), and CKLF1 colocalized with myocardial cells (Figs. 5B and 5E). Moreover, many neutrophils and macrophages infiltrated the infarct area, and CKLF1 colocalized with macrophages and neutrophils (Figs. 5C, 5D, 5F and 5G). This finding suggested that CKLF1 may play a role in chemotaxis to neutrophils and macrophages in the infarct area.

Discussion

In the present study, we demonstrated for the first time a significant increase in CKLF 1 expression after MI in rats, as well as *in vitro* CKLF 1 expression after OGD. *In vivo*, serum CKLF1 levels were significantly elevated on the first-day post-MI but returned to levels similar to those in

the sham group on days 3 and 7. This was comparable to the variations in the serum levels of CK-MB. Compared to that in the sham group, the serum LDH concentration was considerably elevated at 3 days after MI, while there was no significant change at 1 day. In the postinfarction heart, CKLF1 expression was significantly increased in cardiomyocytes, mainly in the infarct margin area. CKLF1 may attract macrophages and neutrophils in rats with myocardial infarction. CKLF1 expression was significantly increased in H9c2 and AC16 cardiomyocytes after OGD *in vitro*.

CKLF1 is a chemokine involved in the pathological processes of various diseases. Patients with atopic dermatitis (AD) have increased CKLF 1 expression in their peripheral blood, and the number of CKLF 1-positive cells is considerably greater in AD skin lesions [16]. Studies using a rat model of cerebral ischemic injury showed that CKLF1 expression was significantly elevated at the site of injury after 3 h and peaked after 48 h. CKLF1 mRNA expression was significantly greater in the peripheral blood of asthmatic patients than in that of controls, and CKLF1 levels in the airways were much greater in asthmatic patients than in those of normal subjects [17]. Patients with rheumatoid arthritis (RA), osteoarthritis (OA), and ankylosing spondylitis (AS) have increased CKLF1 levels in their synovitis [18]. The levels of CKLF1 and CC chemokine

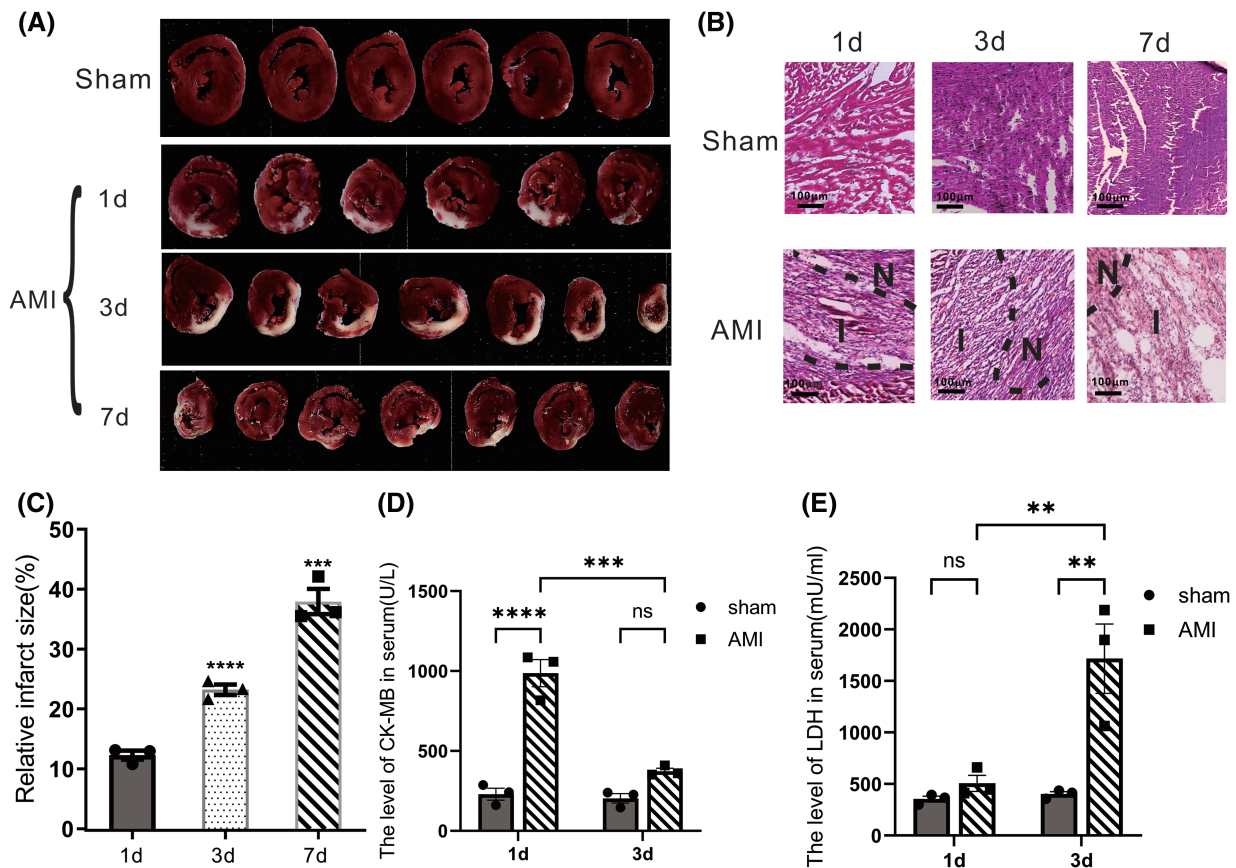


FIGURE 3. An infarction occurred in the left anterior region of the heart in AMI rats. (A and C) TTC staining and statistical analysis. The data are presented as the mean \pm SEM ($n = 3$ rats). (B) HE staining was used for the histological examination of the infarcted tissue. Scale bar = 100 μ m. I: infarct area, N: normal. (D and E) Serum CK-MB and LDH levels at 1 and 3 days after myocardial infarction in rats ($n = 3$ rats). $**p < 0.01$, $***p < 0.001$, $****p < 0.0001$. ns: no statistical significance.

receptor 2 (CCR4) in psoriasis lesions are significantly elevated [19]. Previous research has demonstrated that balloon-damaged rat models of atherosclerosis and human carotid plaques have considerably greater levels of CKLF1 in the neointima following injury than the control group [20]. Compared with normal tissue, hepatocellular carcinoma tissue has much greater CKLF1 expression, and tissues from patients with advanced cancer have greater CKLF1 expression than tissues from patients with early cancer [21]. The amount of CKLF1 increases in rats with abdominal aortic aneurysms [22]. Therefore, CKLF1 overexpression is essential for the pathogenic processes underlying various disorders, suggesting that CKLF1 may be a biomarker for disease diagnosis. Early and precise clinical diagnosis of AMI is critical for patient survival. The major foundation for assessing myocardial hypoxic-ischemic damage is the detection of myocardial enzymes. The two most important cardiac enzyme markers for AMI diagnosis are CK-MB and LDH. Although there was a rise in the serum LDH level 12 to 24 h following AMI-related chest pain, its specificity was not very high. The serum CK-MB concentration might increase 4–6 h after the onset of AMI chest pain and start to decrease after 36 h. Although the sensitivity is great, there are still false positives. When utilized in clinical settings, CK-MB is frequently combined with other cardiac enzymes to increase diagnostic sensitivity and specificity. The results of this investigation showed that the blood levels of CKLF1

dramatically increased one day following AMI before decreasing. CKLF1 is anticipated to serve as a biomarker for the early diagnosis of AMI. CKLF1 antagonists and inhibitors can be used to treat these conditions. Recent research has revealed that conventional inflammatory signaling pathway inhibitors can target CKLF1, control rheumatoid arthritis, and treat cancer [23,24]. Our research demonstrated that increased CKLF1 expression may be crucial to the pathology of myocardial infarction. It is anticipated that CKLF1 will serve as a diagnostic and therapeutic target for myocardial infarction.

CKLF1 has a molecular structure typical of the CC chemokine subfamily. Many studies have shown that members of the CC chemokine subfamily are involved in myocardial infarction. Monocyte chemoattractant protein 1 (MCP-1) and its receptor, CC chemokine receptor 2 (CCR2), have been extensively studied. In the early stages of myocardial infarction, MCP can cause neutrophils and monocytes/macrophages to infiltrate the infarcted area and stimulate the development of collateral arteries [25]. Downregulation of MCP can reduce the expression of tumor necrosis factor- α (TNF- α) and transforming growth factor- β (TGF- β), reduce interstitial fibrosis, and improve ventricular remodeling following infarction [26]. Reduced CCR2 expression can enhance cardiac function following myocardial infarction by decreasing monocyte infiltration, infarct size, and interstitial fibrosis in damaged myocardium

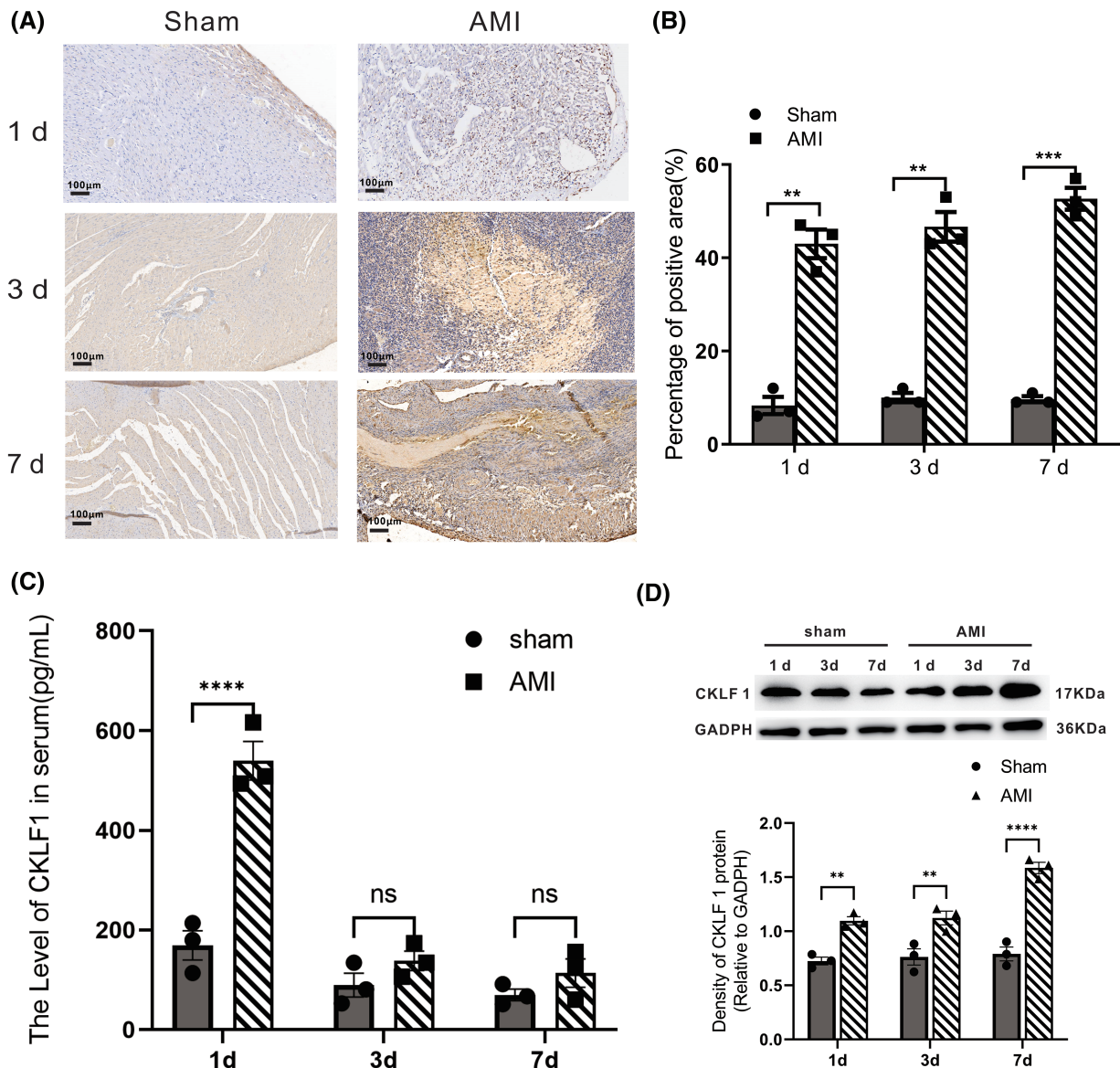


FIGURE 4. The expression of CKLF1 was significantly increased after AMI in rats. (A) Illustrations of representative infarcted and sham-operated heart slices stained with CKLF1 at various time points. Scale bar = 100 µm. (B) Quantification of the area of infarcted and sham-operated hearts stained with CKLF1 at various time points ($n = 3$ rats). (C) The serum CKLF1 concentration of rats was determined by ELISA ($n = 3$ rats). (D) Western blot analysis was used to confirm the presence of the CKLF1 protein in the infarcted area of the rat heart, and ImageJ was used to calculate the protein quantity. The data are presented as the mean \pm SEM ($n = 3$ rats). ** $p < 0.01$, *** $p < 0.001$, **** $p < 0.0001$ vs. the sham group. ns: no statistical significance.

[27]. Thus, ventricular remodeling can be greatly enhanced by MCP/CCR2 downregulation. The biological function of MCP/CCR2 as a pharmacological target to enhance ventricular remodeling following myocardial infarction has drawn the interest of numerous researchers. By using an MCP-1 competitive inhibitor to prevent MCP-1 from binding to the CCR2 receptor, researchers were able to decrease the size of the mouse heart infarct, as well as the amount of collagen and myofibroblasts, monocyte infiltration, and ventricular remodeling [28,29]. After myocardial infarction in mice, silencing CCR2 gene expression with small interfering RNA can improve left ventricular remodeling, minimize monocyte infiltration in the infarct location, and reduce inflammation [30]. CCR2-targeting medications suppress cardiac cell apoptosis induced by ischemia/reperfusion, and pretreatment with targeted therapies can restore decreased

cell viability following ischemia/reperfusion [31]. The results demonstrate that this can considerably decrease the number of monocytes and improve the infarct size and cardiac function in patients with myocardial infarction. Our data showed that CKLF1 was colocalized with cardiomyocytes, macrophages, and neutrophils in the infarct area. The above findings point to the right direction for future research into the mechanism of CKLF1 in myocardial infarction, as well as the potential value of CKLF1 in myocardial infarction treatment.

Adult mammalian cardiomyocytes are not regenerative. Therefore, it is critical to preserve cells in myocardial infarction, particularly those near the border. The area spread outward by at least 3 cm from the infarct location is known as the infarct border zone [32]. The size of the infarct border zone can affect left ventricular remodeling

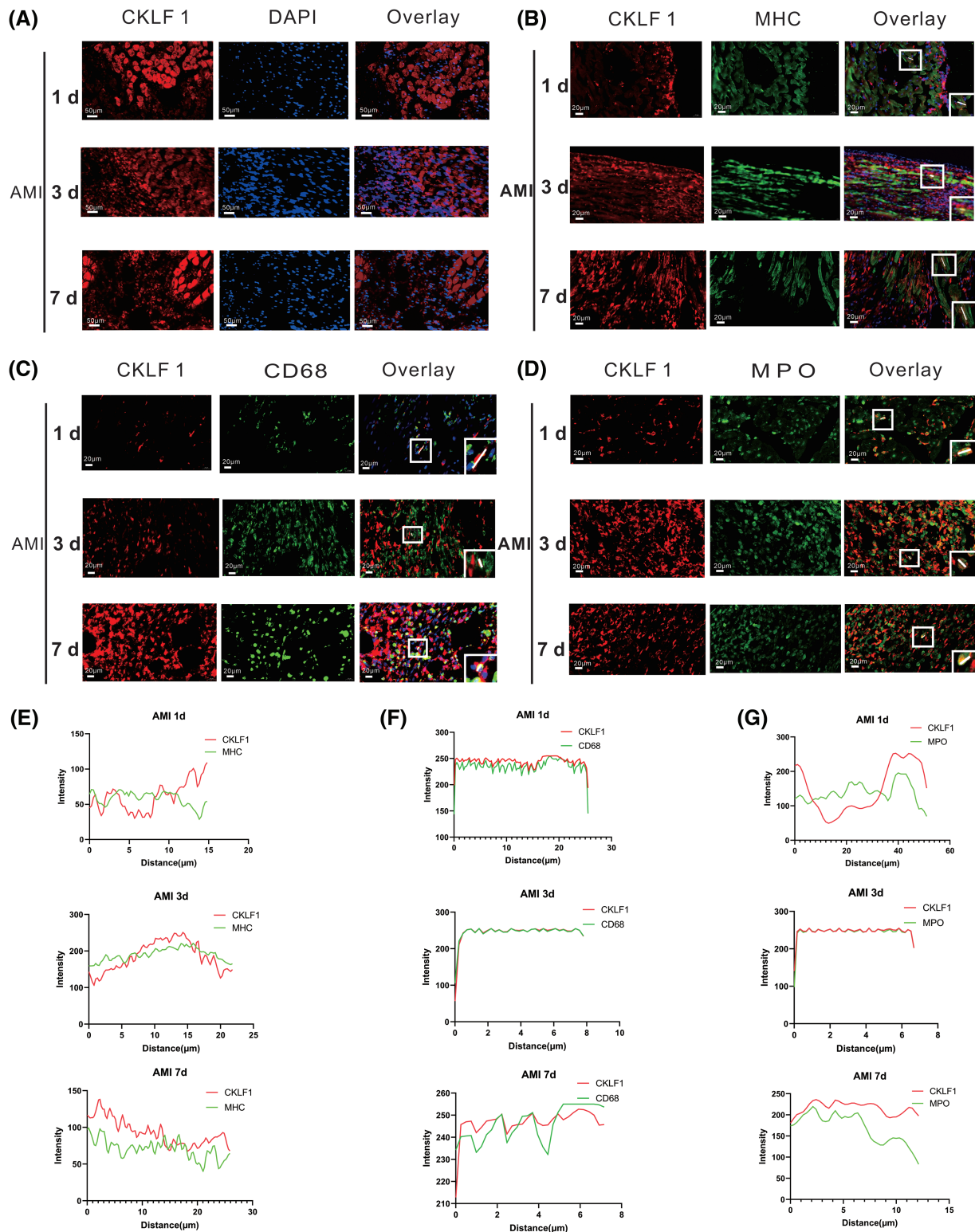


FIGURE 5. CKLF1 expression was increased and colocalized with myocardial cells and inflammatory cells. (A) Immunofluorescence staining of CKLF1 (red) at 1, 3, and 7 days after AMI. Scale bar = 50 μm ($n = 3$). (B and E) Representative photomicrographs of double-staining immunofluorescence and colocalization analysis of CKLF1 (red) and Myosin Heavy Chain (MHC) (green) in the infarcted region at 1, 3, and 7 days after AMI. Scale bar = 20 μm ($n = 3$ rats). (C and F) Representative photomicrographs of double-staining immunofluorescence and colocalization analysis of CKLF1 (red) and CD68 (green) in the infarcted region at 1, 3, and 7 days after AMI. Scale bar = 20 μm ($n = 3$ rats). (D and G) Representative photomicrographs of double-staining immunofluorescence and colocalization analysis of CKLF1 (red) and Myeloperoxidase (MPO) (green) in the infarcted region at 1, 3, and 7 days after AMI ($n = 3$ rats). Scale bar = 20 μm . The lines in the box of the overlay images are the colocalization analysis sites.

and heart failure after myocardial infarction. The mechanisms include the suppression of left ventricular remodeling, electrical remodeling, necrosis, apoptosis, inflammation, and other processes [33–35]. It has been established that suppressing border zone chemokine expression affects ventricular remodeling and myocardial fibrosis [36]. In the border zone of myocardial infarction, macrophages are found near the chemokine CKLF1, which is strongly expressed, according to our findings. The limitations of this study include the lack of in-depth research into the precise mechanism of CKLF1 in myocardial infarction, as well as the inability to adequately explain the function of CKLF1 in myocardial infarction therapy. At the same time, this is the subject of our next study.

Conclusion

The results of the current investigation showed that CKLF1 expression increased significantly in the serum 1 d after myocardial infarction as well as in the infarct tissue, notably in the infarct border zone. Near the infarct, CKLF1 colocalizes with cardiomyocytes, neutrophils, and macrophages.

Acknowledgement: None.

Funding Statement: This work was supported by the National Natural Science Foundation of China (81873026, 82074044, 81900488, and 81730096), the Beijing Natural Science Foundation (7192135), the Health and Family Planning Commission of Hunan Province (202104010694), and the Natural Science Foundation of Hunan Province (2022JJ80028, 2023JJ60369).

Author Contributions: The authors confirm their contribution to the paper as follows: study conception and design: Shifeng Chu, PhD, and Naihong Chen, Prof.; data collection: Haodong Chen, Yangbo Liu; analysis and interpretation of results: Juling Feng, Qidi Ai, Yantao Yang; draft manuscript preparation: Juling Feng, Lei Zhao. All authors reviewed the results and approved the final version of the manuscript.

Availability of Data and Materials: All the data generated or analyzed during this study are included in this article. Further inquiries can be directed to the corresponding authors.

Ethics Approval: All operations were performed by the National Institutes of Health Guide for the Care and Use of Laboratory Animals and were authorized by the Peking Union Medical College and the Chinese Academy of Medical Sciences Animal Care Committee (number: 00007889).

Conflicts of Interest: The authors declare that they have no conflicts of interest to report regarding the present study.

References

- Roth GA, Mensah GA, Johnson CO, Addolorato G, Ammirati E, Baddour LM, et al. Global burden of cardiovascular diseases and risk factors, 1990–2019: update from the GBD, 2019 study. *J Am Coll Cardiol.* 2020;76(25):2982–3021. doi:10.1016/j.jacc.2020.11.010.
- Collaborators GBD. Global burden of 87 risk factors in 204 countries and territories, 1990–2019: a systematic analysis for the global burden of disease study 2019. *Lancet.* 2020;396(10258):1223–49. doi:10.1016/S0140-6736(20)30752-2.
- Shahid M, Rehman K, Akash MSH, Suhail S, Rasheed S, Imran M, et al. Biochemical association between the prevalence of genetic polymorphism and myocardial infarction. *BIOCELL.* 2023;47(3):473–84. doi:10.32604/biocell.2023.025930.
- Karabekir EE, Gultekin K, Orhan K, Onur Y, Nilnur E. Evaluation of the relationship between anti-inflammatory cytokines and adverse cardiac remodeling after myocardial infarction. *Kardiologija.* 2021;61(10):61–70. doi:10.18087/cardio.2021.10.n1749.
- Chen B, Frangogiannis NG. Chemokines in myocardial infarction. *J Cardiovasc Transl Res.* 2021;14(1):35–52. doi:10.1007/s12265-020-10006-7.
- Moser B, Loetscher P. Lymphocyte traffic control by chemokines. *Nat Immunol.* 2001;2(2):123–8. doi:10.1038/84219.
- Francisco J, Del Re DP. Inflammation in myocardial ischemia/reperfusion injury: underlying mechanisms and therapeutic potential. *Antioxid.* 2023;12(11):1944. doi:10.3390/antiox12111944.
- Peet C, Ivetic A, Bromage DI, Shah AM. Cardiac monocytes and macrophages after myocardial infarction. *Cardiovasc Res.* 2020;116(6):1101–12. doi:10.1093/cvr/cvz336.
- Cai X, Deng J, Ming Q, Cai H, Chen Z. Chemokine-like factor 1: a promising therapeutic target in human diseases. *Exp Biol Med.* 2020;245(16):1518–28. doi:10.1177/1535370220945225.
- Yang B, Hong T, Liu QZ, Feng XR, Gong YJ, Bu DF, et al. Effects of *in vivo* transfer of human chemokine-like factor 1 gene on cardiac function after acute myocardial infarction in rats. *Beijing Da Xue Xue Bao Yi Xue Ban.* 2009;41(2):144–7 (In Chinese).
- Feng XR, Hong T, Gong YJ, Bu DF, Yuan JY, Xue L, et al. *In vivo* transfer of human chemokine-like factor 1 gene increases peripheral blood CD34+ stem cells after myocardial infarction in rats. *Beijing Da Xue Xue Bao Yi Xue Ban.* 2006;38(6):592–6 (In Chinese).
- Kong LL, Wang ZY, Han N, Zhuang XM, Wang ZZ, Li H, et al. Neutralization of chemokine-like factor 1, a novel C-C chemokine, protects against focal cerebral ischemia by inhibiting neutrophil infiltration via MAPK pathways in rats. *J Neuroinflammation.* 2014;11:112. doi:10.1186/1742-2094-11-112.
- Chen C, Chu SF, Ai QD, Zhang Z, Chen NH. CKLF1/CCR5 axis is involved in neutrophils migration of rats with transient cerebral ischemia. *Int Immunopharmacol.* 2020;85:106577. doi:10.1016/j.intimp.2020.106577.
- Ai Q, Chen C, Chu S, Luo Y, Zhang Z, Zhang S, et al. IMM-H004 protects against cerebral ischemia injury and cardiopulmonary complications via CKLF1 mediated inflammation pathway in adult and aged rats. *Int J Mol Sci.* 2019;20(7):1661. doi:10.3390/ijms20071661.
- Zhou X, Zhang YN, Li FF, Zhang Z, Cui LY, He HY, et al. Neuronal chemokine-like-factor 1 (CKLF1) up-regulation promotes M1 polarization of microglia in rat brain after stroke. *Acta Pharmacol Sin.* 2022;43(5):1217–30. doi:10.1038/s41401-021-00746-w.
- Yang GY, Chen X, Sun YC, Ma CL, Qian G. Chemokine-like factor 1 (CLFK1) is over-expressed in patients with atopic

- dermatitis. *Int J Biol Sci.* 2013;9(8):759–65. doi:10.7150/ijbs.6291.
17. Tan YX, Han WL, Chen YY, Ouyang NT, Tang Y, Li F, et al. Chemokine-like factor 1, a novel cytokine, contributes to airway damage, remodeling and pulmonary fibrosis. *Chin Med J.* 2004;117(8):1123–9.
 18. Tao K, Tang X, Wang B, Li RJ, Zhang BQ, Lin JH, et al. Distinct expression of chemokine-like factor 1 in synovium of osteoarthritis, rheumatoid arthritis and ankylosing spondylitis. *J Huazhong Univ Sci Technolog Med Sci.* 2016;36(1):70–6. doi:10.1007/s11596-016-1544-4.
 19. Tan Y, Wang Y, Li L, Xia J, Peng S, He Y. Chemokine-like factor 1-derived C-terminal peptides induce the proliferation of dermal microvascular endothelial cells in psoriasis. *PLoS One.* 2015;10(4):e0125073. doi:10.1371/journal.pone.0125073.
 20. Liu X, Qu C, Zhang Y, Fang J, Teng L, Zhang R, et al. Chemokine-like factor 1 (CKLF1) aggravates neointimal hyperplasia through activating the NF- κ B /VCAM-1 pathway. *FEBS Open Bio.* 2020;10(9):1880–90. doi:10.1002/feb4.v10.9.
 21. Liu Y, Liu L, Zhou Y, Zhou P, Yan Q, Chen X, et al. CKLF1 enhances inflammation-mediated carcinogenesis and prevents doxorubicin-induced apoptosis via IL6/STAT3 signaling in HCC. *Clin Cancer Res.* 2019;25(13):4141–54. doi:10.1158/1078-0432.CCR-18-3510.
 22. Li J, Bao X, Li Y, Wang Y, Zhao Z, Jin X. Study of the functional mechanisms of osteopontin and chemokine-like factor 1 in the development and progression of abdominal aortic aneurysms in rats. *Exp Ther Med.* 2016;12(6):4007–11. doi:10.3892/etm.2016.3891.
 23. Ibrahim SSA, Huttunen KM. Orchestrated modulation of rheumatoid arthritis via crosstalking intracellular signaling pathways. *Inflammopharmacol.* 2021;29(4):965–74. doi:10.1007/s10787-021-00800-3.
 24. Degirmenci U, Wang M, Hu J. Targeting Aberrant RAS/RAF/MEK/ERK signaling for cancer therapy. *Cells.* 2020;9(1):198. doi:10.3390/cells9010198.
 25. Zhang H, Yang K, Chen F, Liu Q, Ni J, Cao W, et al. Role of the CCL2-CCR2 axis in cardiovascular disease: pathogenesis and clinical implications. *Front Immunol.* 2022;13:975367. doi:10.3389/fimmu.2022.975367.
 26. Hayashidani S, Tsutsui H, Shiomi T, Ikeuchi M, Matsusaka H, Suematsu N, et al. Anti-monocyte chemoattractant protein-1 gene therapy attenuates left ventricular remodeling and failure after experimental myocardial infarction. *Circ.* 2003;108(17):2134–40. doi:10.1161/01.CIR.0000092890.29552.22.
 27. Jiao J, He S, Wang Y, Lu Y, Gu M, Li D, et al. Regulatory B cells improve ventricular remodeling after myocardial infarction by modulating monocyte migration. *Basic Res Cardiol.* 2021;116(1):46. doi:10.1007/s00395-021-00886-4.
 28. Al-Amran FG, Manson MZ, Hanley TK, Hainz DL. Blockade of the monocyte chemoattractant protein-1 receptor pathway ameliorates myocardial injury in animal models of ischemia and reperfusion. *Pharmacol.* 2014;93(5–6):296–302.
 29. Liehn EA, Piccinini AM, Koenen RR, Soehnlein O, Adage T, Fatu R, et al. A new monocyte chemotactic protein-1/chemokine CC motif ligand-2 competitor limiting neointima formation and myocardial ischemia/reperfusion injury in mice. *J Am Coll Cardiol.* 2010;56(22):1847–57. doi:10.1016/j.jacc.2010.04.066.
 30. Majmudar MD, Keliher EJ, Heidt T, Leuschner F, Truelove J, Sena BF, et al. Monocyte-directed RNAi targeting CCR2 improves infarct healing in atherosclerosis-prone mice. *Circ.* 2013;127(20):2038–46. doi:10.1161/CIRCULATIONAHA.112.000116.
 31. Zhang W, Zhu T, Chen L, Luo W, Chao J. MCP-1 mediates ischemia-reperfusion-induced cardiomyocyte apoptosis via MCP1P1 and CaSR. *Am J Physiol Heart Circ Physiol.* 2020;318(1):H59–71. doi:10.1152/ajpheart.00308.2019.
 32. Lee LC, Wenk JF, Klepach D, Zhang Z, Saloner D, Wallace AW, et al. A novel method for quantifying *in-vivo* regional left ventricular myocardial contractility in the border zone of a myocardial infarction. *J Biomech Eng.* 2011;133(9):94506. doi:10.1115/1.4004995.
 33. Liu S, Li K, Wagner Florencio L, Tang L, Heallen TR, Leach JP, et al. Gene therapy knockdown of Hippo signaling induces cardiomyocyte renewal in pigs after myocardial infarction. *Sci Transl Med.* 2021;13(600):51269.
 34. Tan Y, Bie YL, Chen L, Zhao YH, Song L, Miao LN, et al. Lingbao huxin pill alleviates apoptosis and inflammation at infarct border zone through SIRT1-mediated FOXO1 and NF- κ B pathways in rat model of acute myocardial infarction. *Chin J Integr Med.* 2022;28(4):330–8. doi:10.1007/s11655-021-2881-0.
 35. Fan Y, Cheng Y, Li Y, Chen B, Wang Z, Wei T, et al. Phosphoproteomic analysis of neonatal regenerative myocardium revealed important roles of checkpoint kinase 1 via activating mammalian target of Rapamycin C1/Ribosomal protein S6 Kinase b-1 pathway. *Circ.* 2020;141(19):1554–69. doi:10.1161/CIRCULATIONAHA.119.040747.
 36. Kohno T, Anzai T, Naito K, Sugano Y, Maekawa Y, Takahashi T, et al. Angiotensin-receptor blockade reduces border zone myocardial monocyte chemoattractant protein-1 expression and macrophage infiltration in post-infarction ventricular remodeling. *Circ J.* 2008;72(10):1685–92. doi:10.1253/circj.CJ-08-0115.